

Evaluation of a Functionalized Copolymer as Adsorbent on Direct Dyes Removal Process: Kinetics and Equilibrium Studies

Simona Gabriela Muntean,¹ Oana Paska,² Sergiu Coseri,³ Georgeta Maria Simu,⁴ Maria Elena Grad,¹ Gheorghe Ilia^{1,5}

¹Institute of Chemistry Timisoara of Romanian Academy, 300223 Timisoara, Romania

²Politehnica' University of Timisoara, Faculty of Chemistry and Environmental Engineering, Timisoara, Romania

³Petru Poni' Institute of Macromolecular Chemistry, 700487, Iasi, Romania

⁴University of Medicine and Pharmacy "V. Babes" Timisoara, Faculty of Pharmacy, 300041 Timisoara, Romania

⁵West University, Faculty of Chemistry-Biology and Geography, Timisoara, Romania

Correspondence to: G. Ilia (E-mail: ilia@acad-icht.tm.edu.ro)

ABSTRACT: Functionalized polymeric microbeads were investigated as adsorbent for the removal of three direct dyes from aqueous solutions. The effects of different experimental parameters, such as initial dye concentration, temperature, and solution pH on the adsorption process were investigated. The adsorption process can be conducted with very good result at normal working conditions: neutral pH and normal temperature. The maximum percentage removal obtained was 99.11% for the symmetrical disazo dye, 90.14% for asymmetrical disazo dye, and 98.53% for trisazo dye. The adsorption kinetics followed the pseudo-second-order equation for all three investigated dyes in all working conditions. The experimental data were fitted to Langmuir, Freundlich, Sips, and Redlich–Peterson isotherm models, and the best fit was obtained with Sips model. Thermodynamic parameters (ΔH° , ΔS° , and ΔG°) revealed that dye adsorption is an endothermic and spontaneous process. © 2012 Wiley Periodicals, Inc. *J. Appl. Polym. Sci.* 000: 000–000, 2012

KEYWORDS: direct dyes; functionalized copolymer; kinetics; adsorption isotherm

Received 29 February 2012; accepted 4 May 2012; published online 00 Month 2012

DOI: 10.1002/app.38017

INTRODUCTION

Green chemistry, also called “sustainable chemistry” is a highly effective approach to pollution prevention, which applies innovative scientific solutions to real-world environmental situations. Industries such as textile, paper, plastics, etc., use great quantities of water and chemical substances, for coloring the manufactured articles and discharge large amounts of wastewater during industrial processing. The World Bank estimates that 17–20% of industrial water pollution comes from textile dyeing and treatment. This represents a big environmental problem for the clothing designers and other textile manufacturers. Effluents discharged are aesthetically unpleasant and can produce serious pollution problems.^{1,2} The colored waste waters are considered toxically for aquatic biosphere and affect symbiotic process by reducing the photosynthetic activity.³ For all these reasons, in the recent years, discharge of dye pollutants has become an ecological concern.

Direct dyes widely used in the Romanian textile dyeing industry are water-soluble dyes; they tend to pass through conventional

treatment unaffected so their removal from wastewater is highly difficult. In living organism, some of these dyes can produce carcinogenic and mutagenic aromatic amines in the reductive degradation process, under the action of the enzyme and intestine microflora.^{4,5} International organizations such as International Agency for Research on Cancer (IARC) and Ecological and Toxicological Association of the Dyestuffs Manufacturing (ETAD) developed lists containing aromatic amines with carcinogenic, mutagenic, and teratogenic characteristics.^{6,7} Synthesis of benzidinic direct dyes was forbidden due to the carcinogenic activity of benzidine and the most of its derivatives.^{8,9} In this way finding substitutes for this kind of compounds is an increased demand and a relevant subject. Dyes derived from 4,4'-diaminobenzanilide, are relatively new types of direct dyes, which successfully replace the benzidinic dyes.

In the last years, different methods like coagulation/flocculation,^{10,11} chemical oxidation,¹² extraction,¹³ membrane separation,¹⁴ adsorption,^{15–17} electrochemical reduction,^{18,19} and biodegradation,^{20,21} have been developed to remove the color from dye-containing effluents.²² Among them, adsorption process

Additional Supporting Information may be found in the online version of this article.

© 2012 Wiley Periodicals, Inc.

provides an attractive alternative for the treatment of dye-contaminated waters because of its simplicity, selectivity, and efficiency.²³ Because of their diversity in surface and porosity, high physical-chemistry stability, regeneration and reuse for continuous process, polymeric adsorbents have been used as alternative to activated carbon in removal and recovery of organic pollutants from industrial wastewaters.^{24–28} The dye adsorption is mainly dependent on the dye's structure, and the surface chemistry of the adsorbents, chemical modification being an effective approach for improving adsorption performance of a polymeric adsorbent toward dye removal.^{28–30} Functionalized linear and reticular styrene copolymers can be modified by polymer-analogous reactions in other functional groups.^{31,32} Most of the works published on resin-bound quaternary ammonium salts use styrene-divinylbenzene related resins because of the large amount of technology available on these resins, due to their use as ion exchange resin support. Nevertheless, finding new adsorbents for dyes removal, with high adsorption capacities is still a challenge.²³

The aim of the present work was to investigate the efficiency of a new synthetic modified copolymer, in the removal of three direct dyes from aqueous solutions. For this purpose, equilibrium and kinetic studies have been carried out. The influences of process variables such as time, initial concentration, temperature, and pH have been investigated.

EXPERIMENTAL

Materials

Three types of direct dyes were used as adsorbate: a symmetrical disazo dye (OD), an asymmetrical disazo dye (RD), and a trisazo dye (GD) (Figure 1). The dyes were synthesized in our laboratory to obtain very good substitutes of their benzidinic homologue dyes (C.I. Direct Orange 34, C.I. Direct Red 33, and C.I. Direct Green 9). The synthesis of the studied dyes involved the direct bis-diazotisation of 4,4'-diamino-benzanilide, and the

coupling reactions of bis-diazonium salt with: pyrazolone in case of OD dye³³; salicylic acid and benzoyl I acid for RD dye,³⁴ and in case of GD dye two subsequent coupling reactions: first with salicylic acid, and the second with a monoazo compound prepared by the coupling reaction of the diazonium salt of *p*-nitroaniline with 1-amino-8-hydroxy-3,6-naphthalindisulfonic acid (H acid).³⁵ The dyes were purified by several recrystallizations from distilled water and the dyes purity was around 96%. The dyes were characterized by thin layer chromatography, electronic spectra, and mass spectroscopy.

Chloromethylated styrene-divinylbenzene (*StDVB-ClMe*) used as starting material was supplied by Purolite Victoria Romania (S-6.7% DVB, %Cl 14.22, G_F 4.01 mmol Cl g⁻¹ copolymer). The *StDVB-NMe* resin (Figure 1), was prepared by the polymer-analogous reaction; *StDVB-ClMe* was aminated by adding 25 mL of 25% trimethylamine in ethanol and stirring at room temperature for 24 h. The product was then rinsed with methanol, water, and acetone, and characterized by UV-VIS and FTIR spectroscopy.³⁶

Working solutions were prepared with distilled water to replicate industrial colored wastewaters. The pH values of solutions were adjusted by adding either HCl or NaOH (0.02M), and were measured using a WTW model 330i pH meter.

Physicochemical Determinations

UV-visible absorption spectra of the dyes were recorded using a CECIL CE 7200 Spectrophotometer in the wavelength range 250–750 nm.

The structural characterization of the copolymer microbeads, before and after dye adsorption, was performed by environmental scanning electron microscopy (ESEM) on Quanta 200 instrument. Samples were fixed by means of colloidal silver on copper supports. The samples were covered with a thin layer of gold, by sputtering (EMITECH K 550x). The coated surface was examined by using an Environmental Scanning 200, operating at 5 KV with secondary electrons in High Vacuum Mode.

The estimation of the nitrogen content in the *StDVB-NMe* and dye-attached microbeads has been performed by Energy Dispersive X-ray (EDX) analysis on the Quanta 200 (FEI) electron microscope equipped with EDX system.

The FTIR spectra for the copolymer, the studied dye, and the dye attached to the copolymer microbeads were obtained using a Bruker Vertex 70 instrument. All the spectra were the results of 256 co-added scans at a resolution of 4 cm⁻¹ in KBr pellets, in the range 400–4000 cm⁻¹.

Methods

The adsorption of dyes on the copolymer microbeads has been studied in aqueous solutions in a batch system. For the dye immobilization, 100 mL dye solutions with different concentrations and 0.1 g copolymer were magnetically stirred at 250 rpm for a specific time *t*. After reaching the equilibrium, the colored microspheres were separated through filtration, washed with distilled water (2 × 20 mL), and dried at 313 K for 24 h. The effect of initial concentration of the dye on the adsorption study was carried out using solutions with different dyes

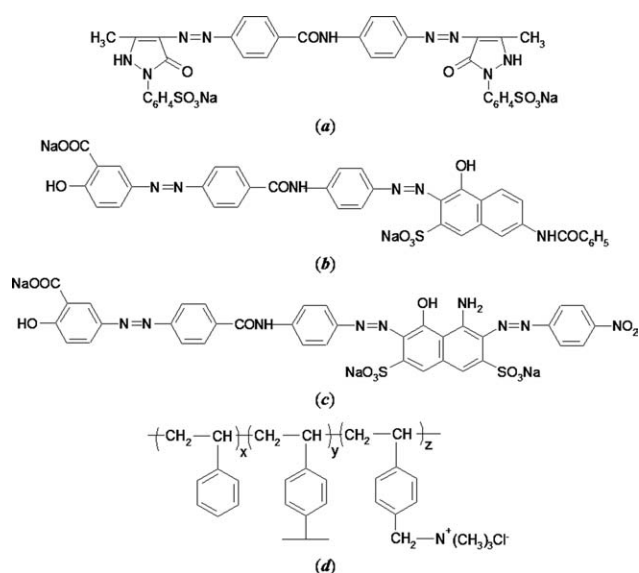


Figure 1. Molecular structure of the: (a) OD (orange), (b) RD (red), (c) GD (green) dyes, and (d) *StDVB-NMe*.

Table I. The Studied Dyes Characteristics

| Dye | Dye formula | Molecular weight (g mol ⁻¹) | λ_{max} ^a (nm) |
|-----|---|---|--|
| OD | C ₃₂ H ₂₅ O ₉ N ₉ S ₂ Na ₂ | 789 | 265; 395 |
| RD | C ₃₇ H ₂₄ O ₉ N ₆ S ₁ Na ₂ | 774 | 382; 515 |
| GD | C ₃₆ H ₂₀ O ₁₃ N ₉ S ₂ Na ₃ | 919 | 380; 625 |

^aMeasured experimentally.

concentrations ranging from 1×10^{-5} to 1×10^{-4} molL⁻¹, at 300 K and pH 7.2. The effect of temperature on the sorption process was studied at three different temperatures (i.e., 303, 318, and 333 K) at pH 7.2. The analysis was extended to various values of solution pH, between 4.1 and 10.4, at 300 K. The pH of the dyes/StDVBNMe system was not controlled during the course of adsorption reaction. In the kinetic experiment, the changes of absorbance were determined at certain time intervals ($0 \div 400$ min) during the adsorption process. The amount of

adsorbed dye per copolymer unit (mg dye g⁻¹ dry copolymer) was calculated using eq. (1):

$$q_t = \frac{(C_0 - C_t) \cdot V}{W} \quad (1)$$

where q_t is the amount of dye adsorbed onto the copolymer unit at time t (mg g⁻¹), C_0 and C_t are the dye concentration in solution at initial time, and at time t (mg L⁻¹), V is the solution volume (L), and W is the amount of adsorbent (g).

The percentage of dye removal (η) was evaluated using eq. (2):

$$\eta = \frac{C_0 - C_e}{C_0} \cdot 100 \quad (2)$$

where C_e is dye concentration at equilibrium (mg L⁻¹).

RESULTS AND DISCUSSION

The chemical structures and the characteristics of the studied dyes are presented in Figure 1 and Table I.

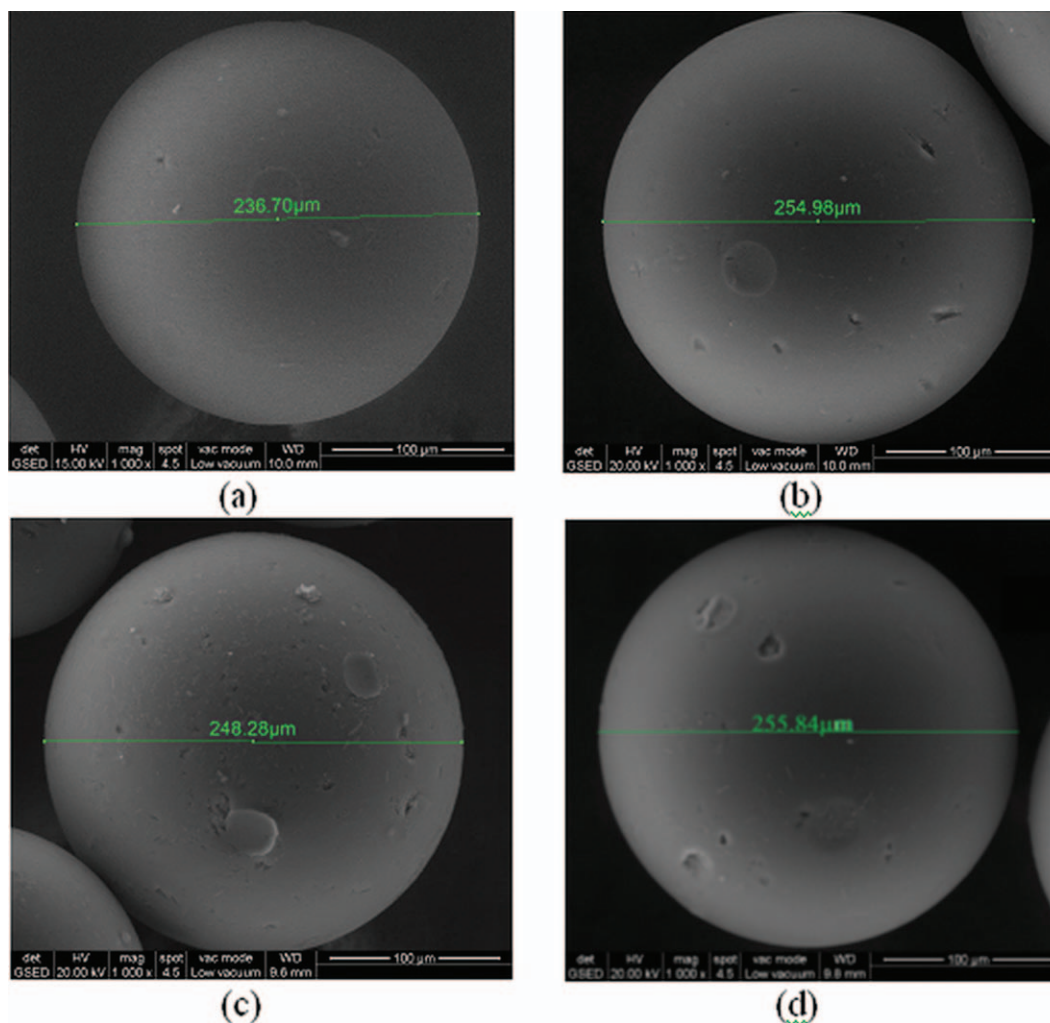


Figure 2. SEM images for (a) StDVB-NMe, (b) StDVB-NMe with OD dye, (c) StDVB-NMe with RD dye, and (d) StDVB-NMe with GD dye. [Color figure can be viewed in the online issue, which is available at wileyonlinelibrary.com.]

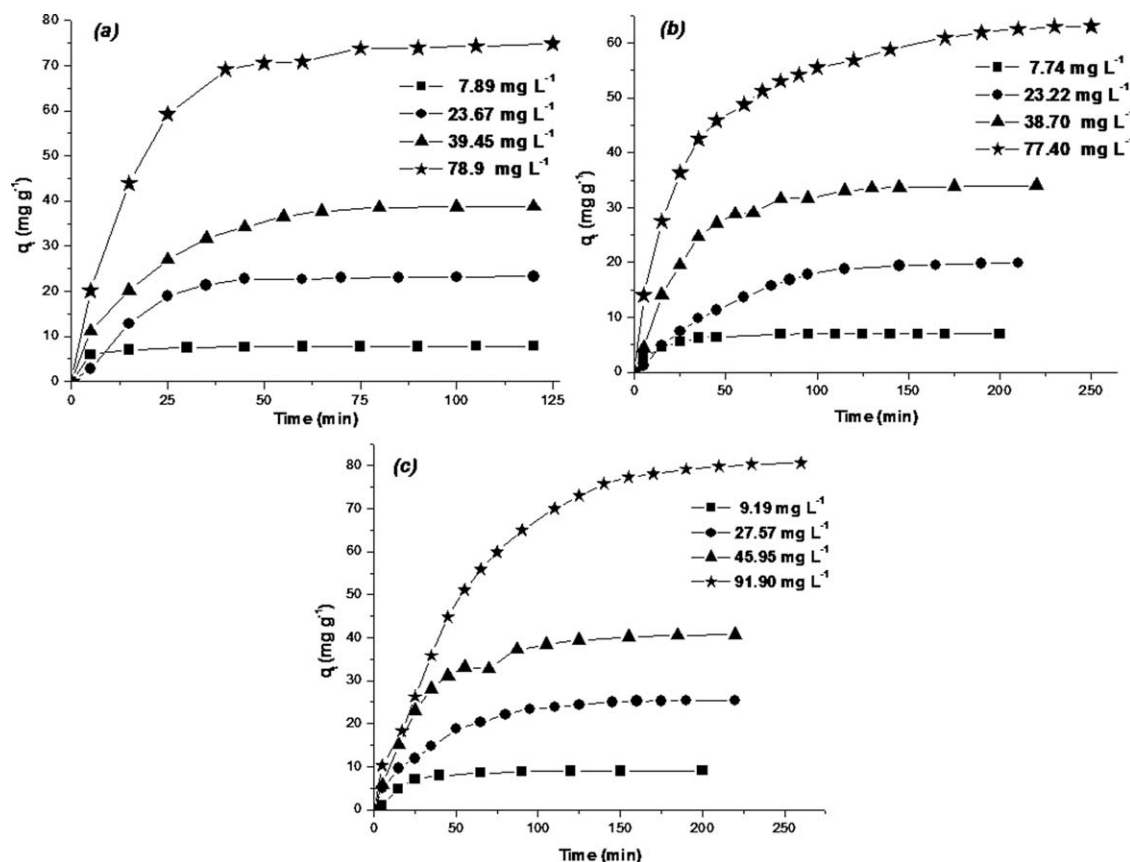


Figure 3. Adsorption of OD (a), RD (b), and GD (c) dyes at different initial concentrations. Conditions: adsorbent dose $100 \text{ mg } 100 \text{ mL}^{-1}$, 300 K , and $\text{pH } 7.2$.

Characterization of Copolymer Microbeads

A synthetic copolymer StDVB-NMe [Figure 1(d)] was investigated as potential adsorbent for the removal of direct dyes. After adsorption process and washing with distilled water, the copolymer microbeads remained uniform colored.

The surface morphology of the StDVB-NMe microbeads, before and after adsorption experiments, was emphasized by electron micrographs (Figure 2). The copolymer has a uniform and spherical form with almost compact structure and smooth surface characteristics.

The elemental analysis of the unmodified StDVB-NMe and dye-attached StDVB-NMe beads were carried out, and the attachment of the dyes were confirmed by an increase of the nitrogen content from 4.9% in starting material to 5.8% in StDVB-NMe with OD dye, 6.9% in StDVB-NMe with RD dye, and 5.4% in StDVB-NMe with GD dye, respectively.

The FTIR spectra showed characteristic bands of nitrogen containing functionalities. The IR spectrum of StDVB-NMe microbeads presents characteristic absorption of aromatic ring in the area of $3000\text{--}3100 \text{ cm}^{-1}$ and a broad peak in the area of $3100\text{--}3600 \text{ cm}^{-1}$ corresponding to the $\text{—CH}_2\text{N}^+\text{Me}_3$ moiety. The evidence of resin amination corresponding to tertiary amine stretching is revealed by the presence of a band at 2782 cm^{-1} .³⁷ The adsorbed dyes onto microbeads copolymer is confirmed by the presence of the $\text{N}=\text{N}$ vibration absorption peak

around 1400 cm^{-1} . The amide group from the dyes, lead to the changes in the $3100\text{--}3500 \text{ cm}^{-1}$ region due to the N—H stretching vibration.

Effect of Initial Dye Concentration and Contact Time

The effect of initial dye concentration and contact time on the adsorption capacity of StDVB-NMe is presented in Figure 3.

For an ecological reason, it is very important to recover dyes from the diluted colored wastewaters. The adsorption is rapid in the initial stages and after reaching the equilibrium time, it remained nearly constant, due to the saturation of the available active centre for dye on the adsorbent surface. The necessary time for reaching the equilibrium increased with increasing the dye concentration, and with increasing the molar mass of investigated dyes $\text{OD} < \text{RD} < \text{GD}$. This is due to the fact that adsorption could occur both at the surface of the polymer, and in the pores of the polymer, and the diffusion of adsorbates into the internal adsorption sites is stimulated by the increasing of the initial dye concentration. The uptake of the studied dyes increased with the increase in initial dye concentration (Figure 3, Table II) while the percentage removal decreased [Figure 4(a)], indicated that the dye removal is concentration dependent, which is in agreement with other reports.^{38,39}

Very good results in the dye removal were obtained at low concentrations: 99.11% for OD, 90.14% for RD, and 98.53% for GD dye, respectively. The results are comparable with values

Table II. Pseudo-First-Order and Second-Order Adsorption Rate Constant, and Comparison of Experimental and Calculated q_e Values for Adsorption of Investigated Dyes on StDVB-NMe

| Conditions | OD | | | | | | RD | | | | | | GD | | | | | |
|---|---|--|--|--|---|---|--|--|--|---|---|--|--|--|---|----------------------------|--|--|
| | First-order kinetic model | | | Second-order kinetic model | | | First-order kinetic model | | | Second-order kinetic model | | | First-order kinetic model | | | Second-order kinetic model | | |
| | $q_{e, \text{exp}}$ (mg g ⁻¹) | $q_{e, \text{calc}}$ (mg g ⁻¹) | $k_1 \times 10^2$ (min ⁻¹) | $q_{e, \text{calc}}$ (mg g ⁻¹) | $k_2 \times 10^3$ (g mg ⁻¹ min ⁻¹) | $q_{e, \text{exp}}$ (mg g ⁻¹) | $q_{e, \text{calc}}$ (mg g ⁻¹) | $k_1 \times 10^2$ (min ⁻¹) | $q_{e, \text{calc}}$ (mg g ⁻¹) | $k_2 \times 10^3$ (g mg ⁻¹ min ⁻¹) | $q_{e, \text{exp}}$ (mg g ⁻¹) | $q_{e, \text{calc}}$ (mg g ⁻¹) | $k_1 \times 10^2$ (min ⁻¹) | $q_{e, \text{calc}}$ (mg g ⁻¹) | $k_2 \times 10^3$ (g mg ⁻¹ min ⁻¹) | | | |
| Conc. ^a (mol L ⁻¹) | | | | | | | | | | | | | | | | | | |
| 1×10^{-5} | 7.82 | 2.49 | 4.53 | 8.33 | 12.38 | 6.99 | 3.23 | 3.39 | 7.31 | 19.15 | 9.06 | 6.30 | 3.42 | 10.26 | 5.04 | | | |
| 3.5×10^{-5} | 23.28 | 20.36 | 5.92 | 27.75 | 2.28 | 19.88 | 25.58 | 2.73 | 17.16 | 0.59 | 25.41 | 21.11 | 2.08 | 29.59 | 1.15 | | | |
| 5×10^{-5} | 38.77 | 48.97 | 6.10 | 45.29 | 1.42 | 34.01 | 21.76 | 1.95 | 38.93 | 1.08 | 40.68 | 32.06 | 2.17 | 46.73 | 0.79 | | | |
| 1×10^{-4} | 74.84 | 58.67 | 4.81 | 83.19 | 1.05 | 63.06 | 50.34 | 2.29 | 68.92 | 0.63 | 80.59 | 83.31 | 1.87 | 82.67 | 0.17 | | | |
| T^b (K) | | | | | | | | | | | | | | | | | | |
| 303 | 37.54 | 21.82 | 3.31 | 39.65 | 2.23 | 31.69 | 21.82 | 3.31 | 39.65 | 2.23 | 34.82 | 30.84 | 1.25 | 36.36 | 0.31 | | | |
| 318 | 38.46 | 12.62 | 2.59 | 40.09 | 2.94 | 34.02 | 12.63 | 2.59 | 40.09 | 2.94 | 40.89 | 32.61 | 2.05 | 43.88 | 1.48 | | | |
| 333 | 39.13 | 6.55 | 3.89 | 39.65 | 3.01 | 36.29 | 6.55 | 3.89 | 39.65 | 10.09 | 42.50 | 47.24 | 2.86 | 42.97 | 1.90 | | | |
| pH ^c | | | | | | | | | | | | | | | | | | |
| 4.1 | 38.32 | 63.27 | 3.04 | 47.37 | 0.37 | 31.40 | 19.36 | 2.10 | 34.36 | 1.39 | 25.94 | 21.23 | 1.78 | 28.02 | 1.12 | | | |
| 7.2 | 38.54 | 23.00 | 3.34 | 40.85 | 2.04 | 34.52 | 20.57 | 1.86 | 37.99 | 1.21 | 36.51 | 45.72 | 1.47 | 35.49 | 0.32 | | | |
| 10.4 | 38.92 | 16.93 | 5.29 | 40.98 | 3.51 | 34.36 | 16.97 | 1.56 | 37.88 | 1.09 | 35.15 | 36.54 | 1.71 | 35.79 | 0.45 | | | |

^aAdsorbent dose 100 mg 100 mL⁻¹, 300 K, and pH 7.2, ^bDye concentration 40 mg L⁻¹, adsorbent dose 100 mg 100 mL⁻¹, 300 K.

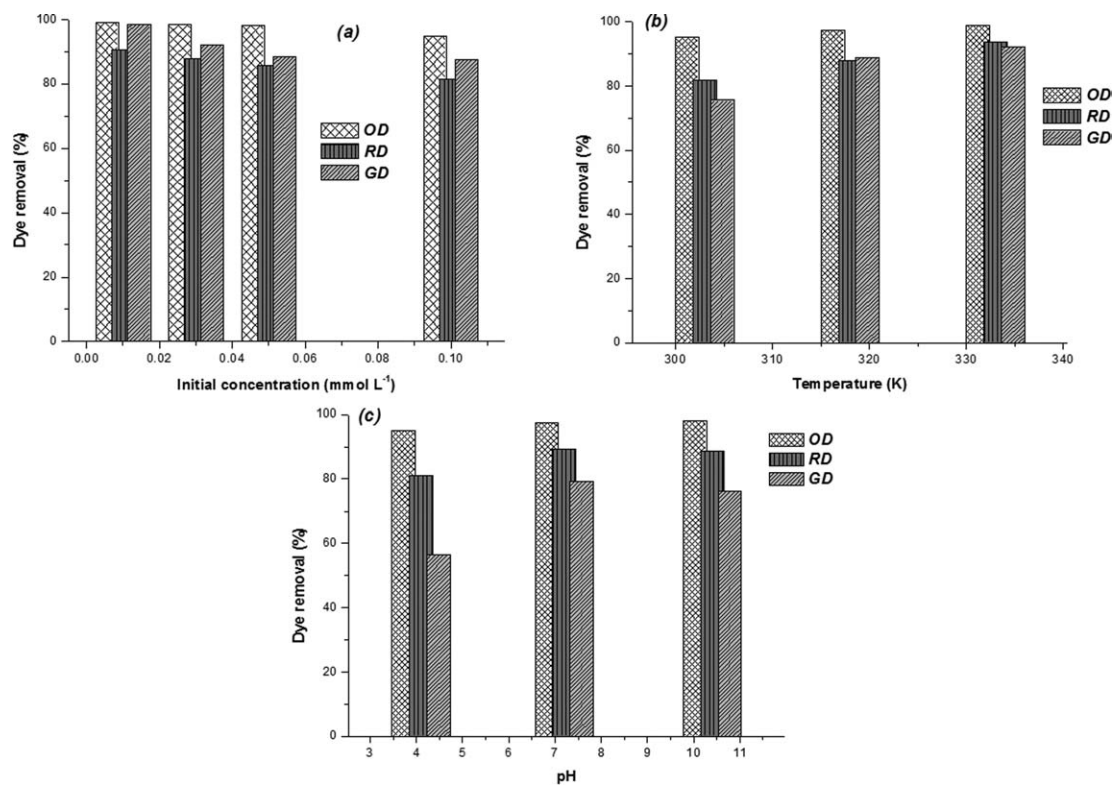


Figure 4. The effect of (a) initial concentration, (b) temperature, and (c) pH on dyes removal percentage.

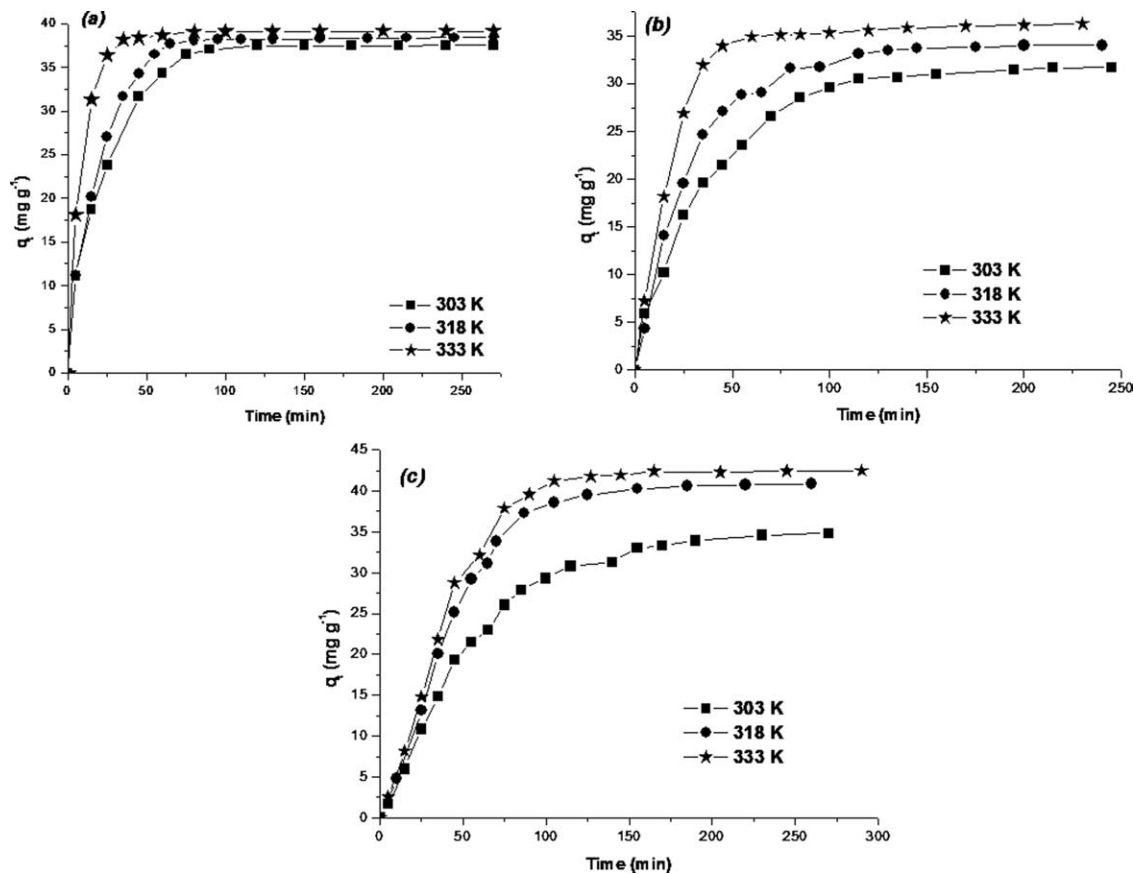


Figure 5. Effect of the temperature on (a) OD, (b) RD, and (c) GD dyes removal. Conditions: dye concentration 40 mg L⁻¹, adsorbent dose 100 mg 100 mL⁻¹, pH 7.2.

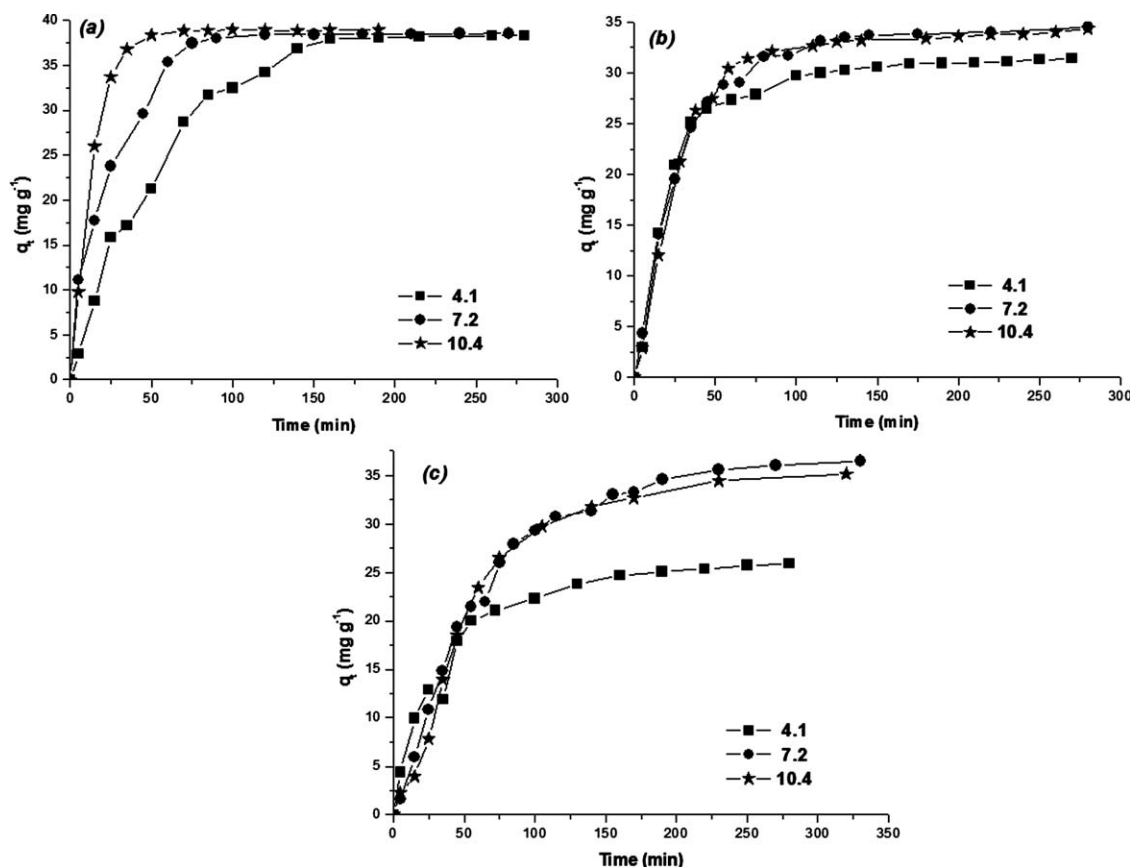


Figure 6. Effect of the solution pH on OD (a), RD (b), and GD (c) dyes adsorption on StDVB-NMe microbeads. Conditions: dye concentration 40 mg L^{-1} , adsorbent dose $100 \text{ mg } 100 \text{ mL}^{-1}$, 300 K .

reported for removal of Acid Green 9 (93%) on acrylic copolymers,¹⁷ DY-12 dye (94.11%),⁴⁰ respectively, direct dyes (97–99%),⁴¹ on activated carbon; or even better than the data reported by: Popa et al. for acid dye (43%) and anthraquinonic dye (24.7%) removal on α -hydroxyphosphonic acid grafted on styrene–divinylbenzene copolymer,³⁰ Kuo et al. for direct dyes removal on carbon nanotubes (51 and 79%, respectively),⁴² Bayramoglu et al.⁴³ for cationic dyes adsorption on p(HEMA-g-GMA) functionalized resin (35 and 74%, respectively), and Coşkun⁴⁴ for cationic dye removal on poly(4-VPy/CrA) resins (27.8–83%). These results clearly demonstrated that StDVB-NMe can be used as a novel alternative adsorbent for the purification of colored wastewaters.

Effect of Temperature

The effect of temperature on the sorption process was studied in the range of $303 \div 333 \text{ K}$, using 100 mg adsorbent dose to 100 mL solution, 40 mg L^{-1} dye concentration, at pH 7.2 (Figure 5). This range of temperatures was chosen to obtain results as closely as possible with normal working conditions, and with minimum working costs.

A comparison of experimental data shows that the increase of temperature induced a positive effect on the sorption capacity in case of the studied dyes, which is in accordance with the data reported by Al-Ghouti et al.⁴⁵ using modified diatomite for dye removal. The increase of the temperature determine an increase

in the adsorption capacity of StDVB-NMe, and the decrease of the necessary time for reaching the equilibrium from 95 to 40 min in case of OD dye, from 120 to 60 min in case of RD dye, and from 210 to 105 min in case of GD dye. The removal percentage of the investigated dyes onto StDVB-NMe, increased from 79.99 to 90.38% (OD), 84.00 to 91.31% (RD) and from 96.58 to 97.91% (GD), with the increase of temperature from 303 to 333 K [Figure 4(b)]. In his work, Hiroyuki explained that the increases of dye removal with the increasing of temperature may be attributed to the chemical reaction taking place between the functional groups of the adsorbate/adsorbent and the dye.⁴⁶

Effect of pH

The pH value of dye solution plays an important role in the whole adsorption process and particularly on the adsorption capacity.^{17,47,48} Most of the dyes are ionic and upon dissociation deliver dye ions into solution. The degree of adsorption of these ions onto the adsorbent surface is primarily influenced by the surface charge on the adsorbent, which in turn it is influenced by the solution pH.²⁹ The effect of pH on dyes removal was investigated in the pH range $4.1 \div 10.4$, to determine the optimum pH value at which the dye removal percentage is maximum. After the pH adjustments, the samples were placed in an oven to sit over night at 303 K ; thereafter the absorption analysis was performed (Figure 6).

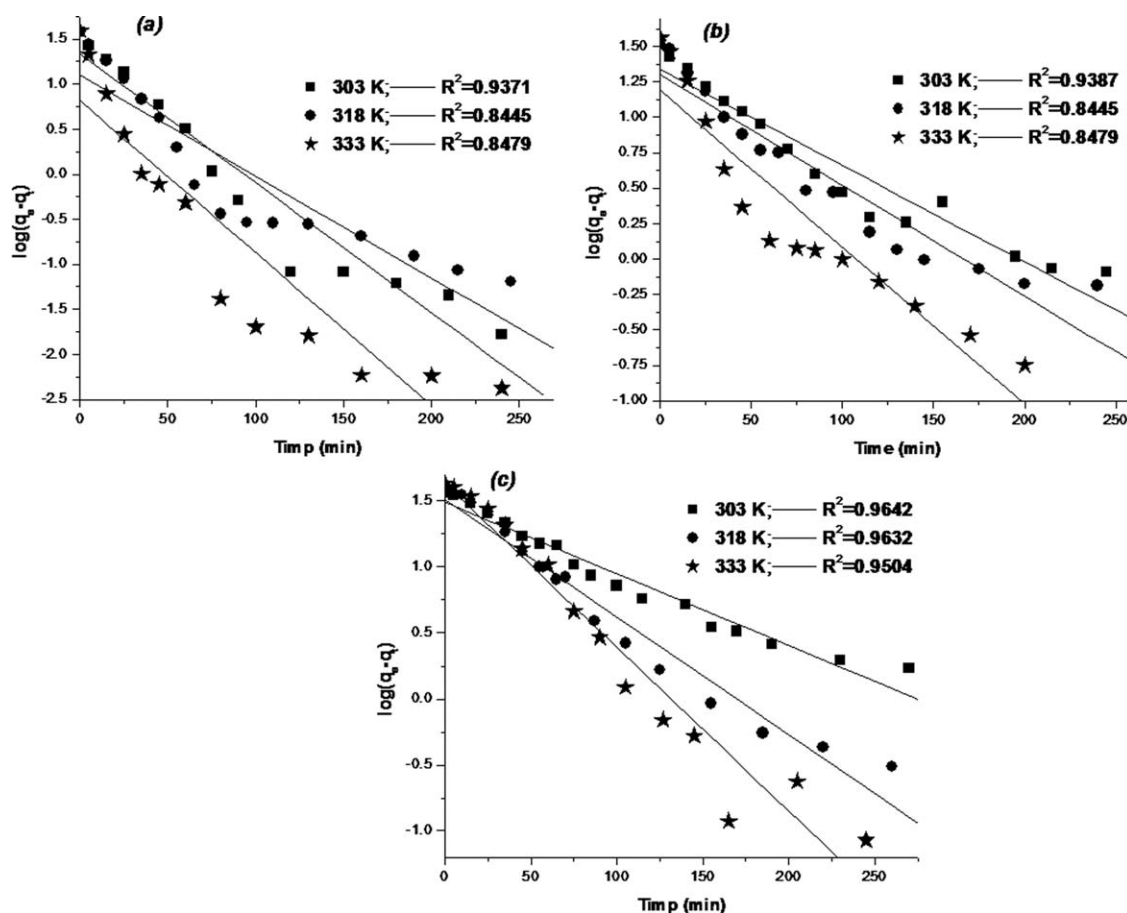


Figure 7. Lagergren plot for the adsorption of OD (a), RD (b), and GD (c) dyes on StDVB-NMe; influence of temperature.

StDVB-NMe is an anion exchange resin with positively charged functional groups ($-\text{NMe}_3^+$) which exchange negatively charged ions. The investigated direct dyes are negatively charged in solution ($-\text{SO}_3^-$, $-\text{COO}^-$), having an affinity to materials with positive charges. In case of OD [Figure 4(c)] the removal percentage (Figure 6) was almost constant for studied pH range, and for RD and GD the adsorption was lower at acidic pH. This behavior could be explained by the differences in chemical structure of the studied dyes. The excess of H^+ promotes protonation of the sulfonic groups of dyes, which are the main groups of the electrostatic interactions adsorbent-dyes in solution. The adsorption of the protonated dyes decreases in relation to the unprotonated ones. With the increase of pH from 4 to 10, an increase in removal percentage was observed for RD and GD dyes. Similar results have been reported by Revathi,⁴⁰ Zohra,⁴⁹ and Verma.⁵⁰ The maximum removal of OD, RD, and GD onto StDVB-NMe resin was found to be at neutral pH [Figure 4(c)]. The higher sorption capacity of the StDVB-NMe obtained at a higher pH may be due to electrostatic attraction between the negatively charged dye molecule, and the positively charged adsorption sites of the sorbent. The slightly lower removal of the studied dyes at higher pH is probably due to the excess of OH^- ions, competing with the anionic dyes (OD, RD, and GD) for the adsorption sites of the sorbent.

Adsorption Kinetics

The adsorption kinetics of all three investigated dyes from aqueous solution on StDVB-NMe microbeads under different conditions has been investigated. The kinetics of adsorption is described by the first-order Lagergren model and pseudo second-order model. The first-order rate expression of Lagergren (3) was used to determine the rate constants k_1 of first-order adsorption:

$$\log(q_e - q) = \log q_e - \frac{k_1}{2.303}t \quad (3)$$

The plot of $\log(q_e - q)$ versus t will give a straight line, and the value of k_1 can be obtained from the slope of the graph.

The second-order kinetic model is expressed as:

$$\frac{t}{q} = \frac{1}{k_2 q_e^2} + \frac{1}{q_e}t \quad (4)$$

where k_2 is the pseudo-second-order adsorption model rate constant ($\text{g mg}^{-1} \text{min}^{-1}$). A plot of t/q as a function of t is linear, and the value of k_2 is determined from the slope and intercept.

The experimental results for influence of temperature were analyzed using the first-order (Figure 7) and pseudo-second-order (Figure 8) models. The kinetic models were fitted using linear

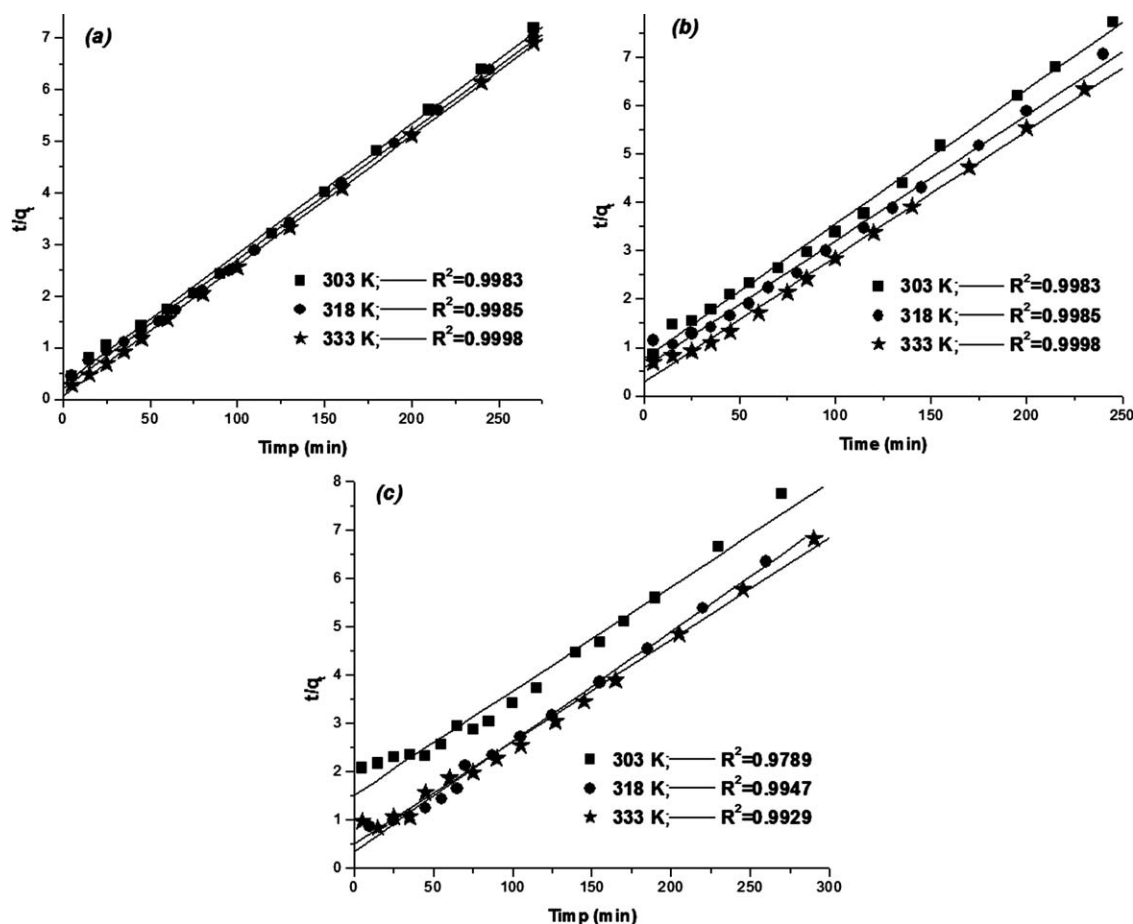


Figure 8. Second-order kinetic model fitting for the adsorption of OD (a), RD (b), and GD (c) dyes on StDVB-NMe; influence of temperature.

fitting method from Origin 6.9 program. The correlation coefficients (R^2) were used to determine the best fitted kinetic model.

The obtained data gave poor fits with the first-order model and very good fits with the pseudo-second-order model as shown by the correlation coefficients. Kinetic studies were made also for the influence of initial concentration and solution pH on the adsorption (Supporting Information). In all cases, the best fit was obtained using the pseudo second-order model.

The comparison of experimental adsorption capacities and the theoretical values, and the computed results estimated from eqs. (3) and (4) are presented Table II.

The theoretical q_e values obtained from the first-order kinetic model for all investigated dyes, in different conditions gave significantly difference from the experimental values, and were very close to the experimental values in case of pseudo-second-order kinetics.

These results showed that the pseudo-second-order kinetic model describes better these adsorbent systems, and that chemical reaction is the main rate-controlling step of the adsorption process. As the temperature was increased, an increase in the pseudo-second-order rate constant k_2 was observed (Table II), indicating that the necessary time for reaching the equilibrium is reduced with increasing temperature.

Adsorption Isotherms

For a better understanding of the adsorption process the equilibrium adsorption studies were carried out. The experimental data obtained at equilibrium, at 318 K, and pH 7.2, were analyzed with Freundlich, Langmuir, Sips, and Redlich–Peterson adsorption models. The Freundlich eq. (5) is the earliest known equation describing the sorption of solutes from a liquid to a solid surface.⁵¹

$$q_e = K_F C_e^{1/n} \quad (5)$$

where K_F is the constant of Freundlich isotherm; n is the Freundlich exponent.

The Freundlich adsorption model stipulates that the ratio of solute adsorbed to the solute concentration is a function of the solution.

Langmuir developed a model based on the assumption that adsorption was a type of chemical combination or process and the adsorbed layer was unimolecular.⁵² Once a dye molecule occupies a site, no further sorption can take place at that site therefore, a saturation value is reached, beyond which no further sorption can take place. The Langmuir equation is expressed as:

$$q_e = \frac{q_m K_L C_e}{1 + K_L C_e} \quad (6)$$

where K_L is the constant of Langmuir isotherm.

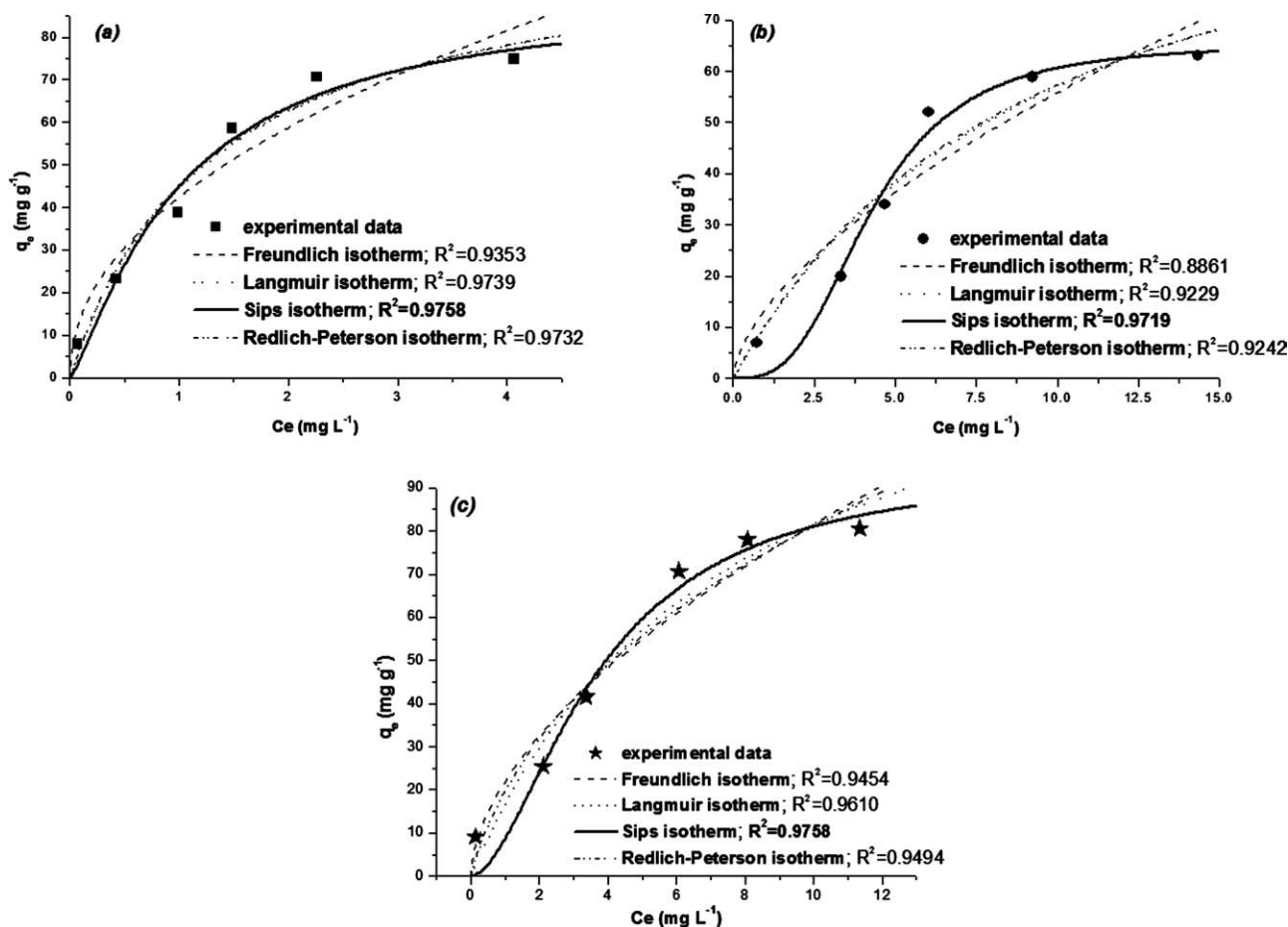


Figure 9. Correlations between experimental data and different types of adsorption isotherms for OD (■), RD (●), and GD (ζ) dye adsorption on StDVB-NMe.

Sips improved the Freundlich and Langmuir equations with a new model which proposes that the equilibrium data follow the Freundlich model at low initial solute concentrations and the Langmuir one at high solute concentrations. In the Sips⁵³ isotherm eq. (7), K_S is the Sips constant related with affinity constant.

$$q_e = \frac{q_m K_S C_e^{1/n}}{1 + K_S C_e^{1/n}} \quad (7)$$

The Redlich–Peterson isotherm unites the Langmuir and Freundlich isotherm, and its adsorption mechanism does not obey ideal monolayer adsorption, but an impure one.⁵⁴ In eq. (8) K_{RP} is the constant of Redlich–Peterson isotherm, α_{RP} is the Redlich–Peterson constant, and β is the Redlich–Peterson exponent ($0 < \beta < 1$).

$$q_e = \frac{K_{RP} C_e}{1 + \alpha_{RP} C_e^\beta} \quad (8)$$

The analysis of the experimental data and determination of the parameters which describes the theoretical models were performed by the ORIGIN version 6.1. Program, principal statistical criteria were the standard deviation (SE) and the squared

Table III. Adsorption Isotherm Constants for the Investigated Dyes Adsorption on StDVB-NMe

| Isotherm | Value | | |
|---|--------|--------|--------|
| | OD | RD | GD |
| Freundlich | | | |
| K_F ($\text{mg g}^{-1}(\text{mg L}^{-1})^{-1/n}$) | 42.42 | 13.53 | 21.87 |
| n | 2.121 | 1.625 | 1.7489 |
| Langmuir | | | |
| q_m (mg g^{-1}) | 104.32 | 114.17 | 143.40 |
| K_L (L mg^{-1}) | 0.7481 | 0.0999 | 0.1318 |
| Sips | | | |
| q_m (mg g^{-1}) | 90.65 | 65.35 | 95.55 |
| K_S ($(\text{mg L}^{-1})^{-1/n}$) | 0.9893 | 0.2345 | 0.2678 |
| N | 0.8015 | 0.3352 | 0.5729 |
| Redlich–Peterson | | | |
| K_{RP} (L g^{-1}) | 81.86 | 11.46 | 35.24 |
| α_{RP} ($\text{mg L}^{-1})^{-\beta}$ | 0.8102 | 0.0918 | 0.7832 |
| β | 0.9887 | 1.0373 | 0.6299 |

Table IV. Thermodynamic Parameters for the Adsorption of OD, RD, and GD on StDVB-NMe Adsorbent

| Dye | T (K) | K_S (L mg ⁻¹) | ΔG^0 (kJ mol ⁻¹) | ΔH^0 (kJ mol ⁻¹) | ΔS^0 (J mol ⁻¹ K ⁻¹) |
|-----|-------|-----------------------------|--------------------------------------|--------------------------------------|---|
| OD | 303 | 0.6001 | -32.92 | 30.35 | 208.62 |
| | 318 | 0.9893 | -35.87 | | |
| | 333 | 2.0815 | -40.2 | | |
| RD | 303 | 0.1091 | -28.58 | 59.54 | 289.78 |
| | 318 | 0.2345 | -32.01 | | |
| | 333 | 1.235 | -38.69 | | |
| GD | 303 | 0.115 | -29.14 | 65.37 | 310.73 |
| | 318 | 0.2678 | -32.82 | | |
| | 333 | 1.65 | -39.99 | | |

multiple regression coefficient (R^2). The comparisons between experimental data and fit sorption isotherm curves are presented in Figure 9. The best isotherm model that fits the experimental data with lower error was the Sips isotherm model.

The adsorption process of investigated dyes is going on after a combined model Freundlich and Langmuir: diffused adsorption on low dye concentration, and a monomolecular adsorption with a saturation value—at high adsorbate concentrations. The data of the fitted models are presented in Table II.

The maximum adsorption capacity of StDVB-NMe for dye removal is more suitable values when compared with the Sips maximum adsorption capacity. From the sorption isotherm curves (saturation value) the maximum adsorption capacity of the StDVB-NMe was determined (Table III); the obtained results are higher or comparable with other published data: 56.2–61.3 mg g⁻¹,⁴² 29.98–37.92 mg g⁻¹,⁵⁵ 20.9–21.6 mg g⁻¹ resin,⁵⁶ and 160 g g⁻¹ resin.⁵⁷

Thermodynamic parameters for the adsorption process were calculated to evaluate the effect of temperature for adsorption of dyes on StDVB-NMe (Table IV). The Gibb's free energy (ΔG^0), was calculated using eq. (9):

$$\Delta G^0 = -RT \ln K_S \quad (9)$$

and enthalpy (ΔH^0), and entropy (ΔS^0) was determined from van't Hoff equation:

$$\ln K_S = \frac{\Delta S^0}{R} - \frac{\Delta H^0}{RT} \quad (10)$$

where R is the universal gas constant (8.314 J K⁻¹ mol⁻¹), T the absolute temperature, and K_S represents the Sips equilibrium constant, obtained from the isotherm plots. ΔH^0 and ΔS^0 values can be calculated from the slope and intercept of the linear plot of $\ln K$ versus $1/T$.

The obtained negative values of ΔG^0 indicate the spontaneous nature of the adsorption process. The increase of temperature determined an increase of ΔG^0 indicating that adsorption is facilitated by higher temperatures. The positive values of ΔH^0 reveal an endothermic nature of adsorption.^{41,58} The positive

value of entropy reflects the increased randomness at the solid-solution interface.

CONCLUSIONS

Adsorption of direct dyes from colored solutions on a new synthetic sorbent was carried out at different working conditions. Adsorption process was quantitative and very fast at low concentrations of the dye solution. The highest dyes removal percent, 99.11% for OD, 90.14% for RD, and 98.53% for GD dye, respectively, was obtained for low concentrations. The increase of temperature determines an increase in adsorption process. The maximum removal percentage of OD, RD, and GD onto StDVB-NMe resin was found to be at neutral pH, highlighting electrostatic attraction between the positively charged adsorption sites of the sorbent, and the negatively charged dyes molecule. Kinetic studies showed that the adsorption followed the pseudo-second-order reaction. The experimental data were well correlated by the Sips adsorption model, and the maximum theoretical adsorption capacities were determined to be 90.65 (OD), 65.35 (RD), respectively, 95.55 (GD) mg g⁻¹ copolymer. The values of thermodynamic parameters, i.e. free energy, enthalpy, and entropy, showed that the adsorption process was spontaneous and facilitated by increasing the temperature. As the adsorption potential of StDVB-NMe microbeads in removing dye molecules is considerable (higher than 90%), it can be used as a new alternative adsorbent for the purification of colored wastewaters. The process can be conducted at normal temperature and neutral pH with minimal working costs, which is important for a potential application in real systems. Work is in progress to explore the application of the new obtained specific sorbents (dye-attached to copolymer microbeads) in removal of heavy metals ions.

NOMENCLATURE

| | |
|-----------|--|
| StDVB-NMe | Styrene-divinylbenzene functionalized with quaternary ammonium groups |
| q_t | Amount of dye adsorbed onto the copolymer unit at time t (mg g ⁻¹) |
| C_0 | Dye concentration in solution at initial time (mg L ⁻¹) |

| | |
|---------------|--|
| C_t | Dye concentration in solution at time t (mg L^{-1}) |
| C_e | Dye concentration at equilibrium (mg L^{-1}) |
| V | Solution volume (L) |
| W | Amount of adsorbent (g) |
| K_1 | Rate constant of first-order adsorption model (min^{-1}) |
| K_2 | Rate constant of pseudo-second-order adsorption model ($\text{g mg}^{-1} \text{min}^{-1}$) |
| T | Time (min) |
| K_F | Constant of Freundlich isotherm ($\text{mg g}^{-1} (\text{mg L}^{-1})^{-1/n}$) |
| N | The Freundlich exponent (dimensionless) |
| K_L | Constant of Langmuir isotherm (L mg^{-1}) |
| K_S | Sips constant related with affinity constant ($(\text{mg L}^{-1})^{-1/n}$) |
| K_{RP} | Constant of Redlich–Peterson isotherm (L g^{-1}) |
| α_{RP} | The Redlich–Peterson constant ($\text{mg L}^{-1})^{-\beta}$ |
| β | The Redlich–Peterson exponent (dimensionless) ($0 < \beta < 1$) |
| q_e | Equilibrium solid phase concentration (mg g^{-1}) |
| $q_{e,cal}$ | Calculated value of solid phase concentration of adsorbate at equilibrium (mg g^{-1}) |
| $q_{e,exp}$ | Experimental value of solid phase concentration of adsorbate at equilibrium (mg g^{-1}) |
| q_m | Maximum adsorption capacity of adsorbent (mg g^{-1}) |

ACKNOWLEDGMENTS

This work was supported by Program 2 of Institute of Chemistry Timisoara of Romanian Academy (Research Project 2.3.). S. Coseri is thankful to POSDRU, project “Social European Fund – Postdoctoral program Cristofor I. Simionescu” – ID 55216. O. Paska is thankful to POSDRU project of the Ministry of Labor, Family and Social Protection, Romania, co-financed by the European Social Fund, Investing in people, ID 107/1.5/S/77265 (2010).

REFERENCES

- Ahmad, A. A.; Hameed, B. H.; Aziz, N. J. *Hazard. Mater.* **2007**, *141*, 70.
- de Aragao Umbuzeiro, G.; Freeman, H. S.; Warren, S. H.; Palma de Oliveira, D.; Terao, Y.; Watanabe, T.; Claxton, L. D. *Chemosphere* **2005**, *60*, 55.
- Edwards, L. C.; Freeman, H. S. *Color. Technol.* **2005**, *121*, 271.
- Pielesz, A.; Baranowska, I.; Rybak, A.; Wlochowicz, A. *Eco-tox. Environ. Safe.* **2002**, *53*, 42.
- Wang, J.; Freeman, H. S.; Claxton, L. D. *Color. Technol.* **2007**, *123*, 39.
- Information Notice No. 6. German Ban of Use of Certain Azo Compounds in Some Consumer Goods; Basel: ETAD, 1998.
- Jäger, I.; Schneider, K.; Janak, P.; Kralove, D.; Huet, M. *Mel-liand International Textile Reports English: 1-2/2005*, *E12*, **2005**.
- Kadlubar, F. F.; Yamazoe, Y.; Lang, N. P.; Chu, D. Z.; Beland, F. A. *Adv. Exp. Med. Biol.* **1986**, *197*, 537.
- Prival, M. J.; Bell, S. J.; Mitchell, V. D.; Peiperl, M. D.; Vaughan V. L. *Mutat. Res.* **1984**, *136*, 33.
- Sadri Moghaddam, S.; Alavi Moghaddam, M. R.; Arami, M. J. *Hazard. Mater.* **2010**, *175*, 651.
- Wang, S.; Yu, D.; Huang, Y.; Guo, J. J. *Appl. Polym. Sci.* **2011**, *119*, 2065.
- Kusic, H.; Peternel, I.; Ukc, S.; Koprivanac, N.; Bolanca, T.; Papic, S.; Bozic, A. L. *Chem. Eng. J.* **2011**, *172*, 109.
- Farizadeh, K.; Montazer, M.; Yazdanshenas, M. E.; Rashidi, A.; Malek, R. M. A. *J. Appl. Polym. Sci.* **2009**, *113*, 3799.
- Criscuoli, A.; Zhong, J.; Figoli, A.; Carnevale, M. C.; Huang, R.; Drioli, E. *Water Res.* **2008**, *42*, 5031.
- Crini, G. *Dyes Pigm.* **2008**, *77*, 415.
- Ahmad, R.; Kumar, R. *Clean* **2011**, *39*, 74.
- Dulman, V.; Simion, C.; Bărsănescu, A.; Bunia, I.; Neagu, V. *J. Appl. Polym. Sci.* **2009**, *113*, 3799.
- Faouzi, A. M.; Nasr, B.; Abdellatif, G. *Dyes Pigm.* **2007**, *73*, 86.
- de Oliveira, G. R.; Fernandes, N. S.; de Melo, J. V.; da Silva, D. R.; Urgeghe, C.; Martínez-Huitle, C. A. *Chem. Eng. J.* **2011**, *168*, 208.
- Pazdzior, K.; Klepacz-Smolka, A.; Ledakowicz, S.; Sojka-Ledakowicz, J.; Mrozinska, Z.; Zylla, R. *Chemosphere* **2009**, *75*, 250.
- Stanescu, M. D.; Sanislav, A.; Ivanov, R. V.; Hirtopeanu, A.; Lozinsky, V. I. *Appl. Biochem. Biotechnol.* **2011**, *165*, 1789.
- Siew-Teng, O.; Pei-Sin, K.; Weng-Nam, L.; Sie-Tiong, H.; Yung-Tse, H. *Water* **2011**, *3*, 157.
- Malarvizhi, R.; Wang, M. H.; Ho, Y. S. *World Appl. Sci. J.* **2010**, *8*, 930.
- Sandic, Z. P.; Nastasovic, A. B.; Jovic-Jovicic, N. P.; Milutinovic-Nikolic, A. D.; Jovanovic, D. M. J. *Appl. Polym. Sci.* **2011**, *121*, 234.
- Bărsănescu, A.; Buhăceanu, R.; Dulman, V. J. *Appl. Polym. Sci.* **2009**, *113*, 607.
- Luo X, Zhan Y, Huang Y, Yang L, Tu X, Luo S. J. *Hazard. Mater.* **2011**, *187*, 274.
- Arslan, M. J. *Appl. Polym. Sci.* **2011**, *119*, 3034.
- Singh, V.; Sharma, A. K.; Tripathi, D. N.; Sangh, R. J. *Hazard. Mater.* **2009**, *161*, 955.
- Qiu, Y.; Ling, F. *Chemosphere* **2006**, *64*, 963.
- Popa, A.; Muntean, S. G.; Paska, O. M.; Iliescu, S.; Ilia, G.; Zhang, Z. *Polym. Bull.* **2011**, *66*, 419.
- Gao, Y.; Cranston, R. *Text. Res. J.* **2008**, *78*, 60.
- Alexandratos, S. D. *Ind. Eng. Chem. Res.* **2009**, *48*, 388.
- Grad, M.; Simu, G.; Hora, S.; Chicu, S. A.; Şişu, E. *Chem. Bull. “Politehnica” Univ. (Timişoara)* **2004**, *49*, 31.
- Simu, G. M.; Funar-Timofei, S. L.; Hora, S. G.; Schmidt, W.; Kurunczi, L.; Sisu, E.; Morin, N. *Rev. Chim. Bucharest* **2002**, *53*, 826.
- Simu, G.; Funar-Timofei, S.; Hora, S.; Kurunczi, L. *Mol. Cryst. Liq. Cryst.* **2004**, *416*, 97.

36. Muntean, S.; Simu, G.; Grad, M.; Moldovan, R. In Proceedings of 140 Years from Establishment of Romanian Academy, **2006**, p 185.
37. Qiu, Y. P.; Chen, J. L.; Li, A. M.; Zhang, Q. X.; Huang, M. S. *Chin. J. Polym. Sci.* **2005**, *23*, 435.
38. Amin, N. K. *J. Hazard. Mater.* **2009**, *165*, 52.
39. Khan, T.; Chaudhuri, M. *Res. J. Chem. Environ.* **2011**, *15*, 601.
40. Revathi, G.; Ramalingam, S.; Subramaniam, P.; Ganapathie, A. E. *J. Chem.* **2011**, *8*, 1536.
41. Yavuz, Ö.; Aydin, A. H. *Pol. J. Environ. Stud.* **2006**, *15*, 155.
42. Kuo, C. Y.; Wu, C. H.; Wuc, J. Y. *J. Coll. Interf. Sci.*, **2008**, *327*, 308.
43. Bayramoglu, G.; Altintas, B.; Arica, M. Y. *Chem. Eng. J.* **2009**, *152*, 339.
44. Coşkun, R. *Polym. Bull.* **2011**, *67*, 125.
45. Al-Ghouti, M.; Khraisheh, M. A. M.; Ahmad, M. N. M.; Allen, S. J. *Coll. Interf. Sci.* **2005**, *287*, 6.
46. Hiroyuki, H.; Fukuda, S.; Okamoto, A.; Kataoka, T. *Chem. Eng. Sci.* **1994**, *48*, 2267.
47. Royer, B.; Cardoso, N. F.; Lima, E. C.; Ruiz, V. S.O.; Macedo, T. R. Airoidi, C. J. *Coll. Interf. Sci.* **2009**, *336*, 398.
48. Mahmoodi, N. M.; Arami, M.; Bahrami, H.; Khorramfar, S. *J. Appl. Polym. Sci.* **2011**, *120*, 2996.
49. Zohra, B.; Aicha, K.; Fatima, S.; Nourredine B.; Zoubir, D. *Chem. Eng. J.* **2008**, *136*, 295.
50. Verma, V. K.; Mishra, A. K. *Global NEST J.* **2010**, *12*, 190.
51. Freundlich, H. Z. *Phys. Chem.* **1907**, *57*, 385.
52. Langmuir, I. *J. Am. Chem. Soc.* **1918**, *40*, 1361.
53. Sips, R. J. *Chem. Phys.* **1948**, *16*, 490.
54. Redlich, O.; Peterson, D. L. *J. Phys. Chem.* **1959**, *63*, 1024.
55. Safa, Y.; Bhatti, H. N. *Afr. J. Biotechnol.* **2011**, *10*, 3128.
56. Zhang, X.; Li, A.; Jiang, Z.; Zhang, Q. *J. Hazard. Mater.* **2006**, *B137*, 1115.
57. Kaner, D.; Saraç, A.; Şenkal, F. B. *Environ. Geochem. Health* **2010**, *32*, 321.
58. Li, Q.; Yue, Q. Y.; Sun, H. J.; Su, Y.; Gao B. Y. *J. Environ. Manage.* **2010**, *911601*.